The Astrophysical Journal, 629:L53–L56, 2005 August 10


# MEASUREMENTS OF $CH_3D$ AND $CH_4$ IN TITAN FROM INFRARED SPECTROSCOPY

P. F. Penteado and C. A. Griffith
Lunar and Planetary Laboratory and Department of Planetary Sciences, University of Arizona, 1629 East University Boulevard, Tucson, AZ 85721-0092; penteado@lpl.arizona.edu, griffith@lpl.arizona.edu
T. K. Greathouse
Lunar and Planetary Institute, 3600 Bay Area Boulevard, Houston, TX 77058-1113; greathouse@lpi.usra.edu
and
C. de Bergh
LESIA, Observatoire de Paris, 92195 Meudon, France; catherine.debergh@obspm.fr
*Received 2005 January 14; accepted 2005 June 28; published 2005 July 21*

## ABSTRACT

We measured the $CH_4$ column abundance in Titan's atmosphere through an analysis of Titan's monodeuterated methane ($CH_3D$) spectral features. $CH_3D$ is several orders of magnitude less abundant in Titan's atmosphere than $CH_4$. Thus, unlike $CH_4$, the strong and well-studied $CH_3D$ $3\nu_2$ lines are not saturated and provide a sensitive measure of its column abundance. We recorded the $CH_3D$ $3\nu_2$ lines at 1.55 $\mu$m at NASA's Infrared Telescope Facility (IRTF) equipped with the Cryogenic Echelle Spectrograph. We derive a total integrated column abundance of 2.1 $\pm$ 0.1 m amagat for $CH_3D$. We also measured stratospheric emission lines of both $CH_3D$ and $CH_4$ at 8.6 $\mu$m at higher resolution than previously possible to better constrain the $CH_3D/CH_4$ ratio. These observations, recorded at the IRTF using the Texas Echelon Cross Echelle Spectrograph, were analyzed with radiative transfer calculations. We determine a $CH_3D/CH_4$ ratio of $(50 \pm 10) \times 10^{-5}$. Taken together, our measurements of the $CH_3D$ column abundance and the $CH_3D/CH_4$ ratio indicate a total $CH_4$ column abundance of $4.2^{+1.3}_{-0.9}$ km amagat, close to the column abundance of an atmosphere with 100% saturation in the entire troposphere.

*Subject heading:* planets and satellites: individual (Titan)

## 1. INTRODUCTION

In Titan's atmosphere, methane ($CH_4$) is the second most abundant substance detected and one of the main greenhouse gases (McKay et al. 1989, 1991). Recent observations of transient clouds (Griffith et al. 1998, 2000; Roe et al. 2002; Brown et al. 2002) and evidence for liquid reservoirs on the surface (Campbell et al. 2003) suggest that its abundance in the lower atmosphere may be controlled by a cycle similar to that of water on Earth. In spite of its recognized importance, there are conflicting measurements of the total methane content in the atmosphere (Courtin et al. 1995; Lemmon et al. 2002). Spectroscopic measurements are complicated by the fact that Titan's high methane column density saturates its strong bands, while the nonsaturated lines are difficult to measure in the laboratory. The current *Cassini* mission will determine the methane abundance at the *Huygens Probe* landing site using the Gas Chromatograph Mass Spectrometer (GCMS; Niemann et al. 2002). However, the determination of the variation of the methane abundance across Titan's disk will require spectroscopic measurements.

In this work we study the possibility of using strong and well-studied $3\nu_2$ band lines of monodeuterated methane ($CH_3D$) at 1.55 $\mu$m in Titan's spectrum to infer the total methane abundance. Since they are much weaker than $CH_4$ lines, the $CH_3D$ lines provide a good estimate of the total column abundance, where they are not blended with $CH_4$ lines. The total methane abundance is then inferred from estimates of the $CH_3D/CH_4$ isotopic ratio. We use Titan's emission lines of the $CH_4$ and $CH_3D$ $\nu_4$ band at better resolution than previously possible to estimate the $CH_3D/CH_4$ isotopic ratio.

Coustenis et al. (1989) analyzed *Voyager 1* spectra of the 8.6 $\mu$m $CH_3D$ band to measure an isotopic ratio of $60^{+56}_{-22} \times 10^{-5}$. Orton (1992) also recorded the 8.6 $\mu$m band with observations from IRTF and found that the temperature uncertainties did not strongly influence the inferred isotopic ratio of $CH_3D/CH_4 = (31 \pm 9) \times 10^{-5}$. The most recent observations of the $\nu_4$ $CH_3D$ band were made with the *Infrared Space Observatory* (*ISO*; Coustenis et al. 2003), and they indicate an isotopic ratio of $35^{+13}_{-7.6} \times 10^{-5}$.

Considering Titan's near-IR spectrum, de Bergh et al. (1988) identified and analyzed two $3\nu_2$ features where the $CH_3D$ contributions are most clearly distinct from those of $CH_4$. A $CH_3D/CH_4$ ratio of $66 \times 10^{-5}$ best fit the data. Trafton (1975) estimated Titan's methane column abundance to be 1.6 km amagat, using spectra of the $3\nu_3$ band of $CH_4$. Fink & Larson (1979) compared spectra of Saturn, Titan, Uranus, and Neptune at 0.8–2.5 $\mu$m and estimated from the 1.3 and 1.6 $\mu$m bands an abundance of 1 km amagat. With the refractivity profiles from *Voyager 1* and spectra of the 1.1 $\mu$m absorption band of $CH_4$, Lellouch et al. (1992) found a column abundance of 4 km amagat.

Lemmon et al. (2002) measured the $CH_4$ absorption bands in the region 0.6–1.1 $\mu$m, with the band curves of growth derived from laboratory data and spectra of Jupiter, Saturn, Titan, Uranus, and Neptune by Karkoschka (1998). As haze scattering increases the optical path transversed by the radiation, a maximum column abundance of 3.5 km amagat was derived assuming no haze, while their haze model resulted in a column abundance of only 2.63 $\pm$ 0.17 km amagat. Tables 1 and 2 summarize the current estimates of the isotopic ratio and total methane column density.

## 2. OBSERVATIONS

Near-infrared observations were recorded on 2001 November 13 at the IRTF, using the Cryogenic Echelle Spectrograph (CSHELL; Greene et al. 1993). Spectra were obtained in five adjacent intervals and later combined in a spectrum covering the entire 1.542–1.560 $\mu$m region with a nominal resolving power of 20,000. For each interval, 12 5 minute exposures were taken of Titan and 12 30 s exposures of the solar analog G4 V star HR 1656 (HD 32923), which was used to obtain a reflection

TABLE 1
DETERMINATIONS OF THE $CH_3D/CH_4$ RATIO

| Wavelength | Instruments | Resolution | $CH_3D/CH_4$ | Ref. |
|---|---|---|---|---|
| 8.6 $\mu$m ..... | KPNO 2.1 m and 4 m | 50 | $1.1 \times 10^{-5}$ | 1 |
| | KPNO 2.1 and 4 m, IRTF, *Voyager* IRIS | 50, 66, 250 | $170 \times 10^{-5}$ | 2 |
| | *Voyager* IRIS | 250 | $60^{+56}_{-22} \times 10^{-5}$ | 3 |
| | IRTF IRSHELL | 10000 | $(31 \pm 9) \times 10^{-5}$ | 4 |
| | *ISO* SWS | 1900 | $35^{+13}_{-7.6} \times 10^{-5}$ | 5 |
| 1.6 $\mu$m ..... | 4 m KPNO FTS | 5400 | $66^{+60}_{-30} \times 10^{-5}$ | 6 |
| 8.6 $\mu$m ..... | IRTF TEXES | 70000 | $(50 \pm 10) \times 10^{-5}$ | 7 |

REFERENCES.—(1) Gillet 1975; (2) Kim & Caldwell 1982; (3) Coustenis et al. 1989; (4) Orton 1992; (5) Coustenis et al. 2003; (6) de Bergh et al. 1988; (7) this work.

spectrum. The flux was calibrated to match a reference spectrum recorded on 1999 September 23 at the United Kingdom Infrared Telescope (UKIRT) with the Cooled Grating Spectrometer (Griffith et al. 2000), which closely matches our observing geometry. This reference spectrum covers 1.45–2.1 $\mu$m, with a resolving power of ~330. Our final calibrated spectrum has an estimated 1 $\sigma$ noise level of 0.5%.

On 2001 November 16 we recorded emission spectra of $CH_4$ and $CH_3D$ with the Texas Echelon Cross-dispersed Echelle Spectrograph (TEXES; Lacy et al. 2002) at the IRTF. The spectra have a resolving power of $R = 70{,}000$ and extend from 1151.8 $cm^{-1}$ (8.6819 $\mu$m) to 1159.8 $cm^{-1}$ (8.6222 $\mu$m). The asteroid 4 Vesta was also observed, and after the pipeline reduction, the final spectrum of Titan was divided by that of Vesta to eliminate the effects of telluric absorption, and flux-calibrated to match the spectrum of Orton (1992). The main lines in the resulting spectrum are shown in Figure 1.

We recorded the observations shortly before Titan's northern winter solstice (on 2002 October). The sub-Earth point was at latitude $-25\overset{\circ}{.}6$. The sub-Earth longitude was 336°–340° for the 1.56 $\mu$m observations and 44°–45° for the 8.6 $\mu$m observations. All spectra sample Titan's entire disk.

## 3. ANALYSIS OF TITAN'S INFRARED SPECTRUM

Titan's 1.6 $\mu$m spectrum contains both $CH_4$ and $CH_3D$ lines. However, as a result of the uncertainties of the $CH_4$ absorption coefficients, a reliable $CH_4$ abundance cannot be derived. Therefore, we analyzed the data to constrain only the $CH_3D$ column abundance. Titan's 1.6 $\mu$m spectrum also depends on the surface reflection and haze scattering. These properties were determined by analyzing the UKIRT spectrum at 1.58 $\mu$m, where the atmosphere is most transparent, to obtain the surface albedo, and at 1.63–1.73 $\mu$m, where haze most strongly affects the observed spectrum. The $CH_4$ lines in the 1.55 $\mu$m region were then fit by varying the $CH_4$ vertical profile. These absorption features provide a continuum for the $CH_3D$ lines, which were then fit to determine the $CH_3D$ abundance.

Spectra at 1.6 $\mu$m were calculated by approximating the radiative transfer equation with a discrete ordinates algorithm (Stamnes et al. 1988). We resolve the atmosphere into parallel layers of constant temperature, pressure, and composition and calculate the scattering and absorption of sunlight at each layer. The spectrum is determined at 21 different air masses, from the center of the disk to the limb, and integrated to obtain a spectrum of the entire disk.

The model assumes the equatorial temperature-pressure profile determined from *Voyager* radio occultation measurements and Infrared Radiometer Interferometer and Spectrometer (IRIS) spectra (Lellouch et al. 1989). Titan's 1.58 $\mu$m spectrum indicates a surface albedo of 0.15 (Griffith et al. 2000). We approximated the scattering properties of the haze by assuming brightly scattering spherical particles with radii 0.3 $\mu$m. We first assumed that the haze density follows the pressure scale height (consistent with Titan's infrared spectrum of Samuelson 1983). Then the haze profile was further adjusted to match Titan's 1.63–1.73 $\mu$m albedo to the UKIRT spectrum, as discussed in Griffith et al. (2000). The fit for the 1.55 $\mu$m continuum for the $CH_3D$ lines was obtained by varying only the $CH_4$, by changing the condensation level between 100% and 200% saturation, and the surface humidity between 30% and the condensation level. The $CH_3D$ was then varied to fit the $CH_3D$ lines.

For $CH_3D$, at 1.55 $\mu$m, we calculated the line intensities and energy levels using the coefficients from Boussin et al. (1998, 1999) and Lutz et al. (1983). To model the $CH_4$ lines in Titan and Uranus at 1.55 $\mu$m, de Bergh et al. (1986, 1988) used spectra of Saturn as the reference cold spectrum. Saturn's spectra were analyzed with a radiative transfer model, and once a best fit was found the remaining differences were attributed to errors in the populations of the energy levels. The values for the $J$ quantum numbers were then changed to match the re-

TABLE 2
DETERMINATIONS OF THE $CH_4$ TOTAL COLUMN ABUNDANCE

| Data | Instruments | Column Density (km amagat) | Ref. |
|---|---|---|---|
| $CH_4$ abs. at 0.5–1.2 $\mu$m ..... | 2.7 m McDonald telescope | 1.6 | 1 |
| $CH_4$ abs. at 0.8–2.5 $\mu$m ..... | 4 m KPNO | 1 | 2 |
| $CH_3D$ abs. at 1.6 $\mu$m ..... | 4 m KPNO FTS | 2.2 | 3 |
| Refractivity and $CH_4$ abs. at 7.7 $\mu$m ..... | *Voyager* RSS and IRIS | 0.4–3.0, <6.9 | 4 |
| $CH_4$ abs. at 1.1 $\mu$m ..... | IRTF (CGAS) and CFH (FTS) | $4 \pm 1$ | 5 |
| Refractivity and abs. at 16–50 $\mu$m ..... | Voyager RSS and IRIS | 2.3–4.0 | 6 |
| $CH_4$ abs. at 0.3-1.1 $\mu$m ..... | *HST* STIS | $2.63 \pm 0.17$, <3.5 | 7 |
| $CH_3D$ abs. at 1.6 $\mu$m and $CH_3D/CH_4$ emiss. at 8.6 $\mu$m ..... | IRTF (CSHELL and TEXES) | $4.2^{+1.3}_{-0.9}$ | 8 |

REFERENCES.—(1) Trafton 1975; (2) Fink & Larson 1979; (3) de Bergh et al. 1988; (4) Lellouch et al. 1989; (5) Lellouch et al. 1992; (6) Courtin et al. 1995; (7) Lemmon et al. 2002; (8) this work.

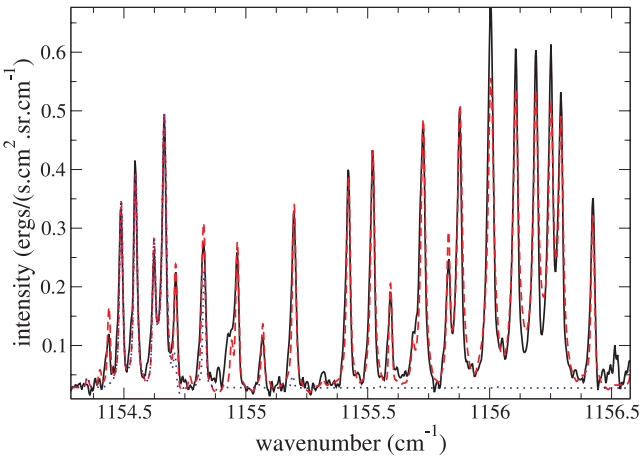


FIG. 1.—Titan's emission spectrum at the main $CH_3D$ and $CH_4$ bands. *Black solid line*: Observed spectrum. *Red dashed line*: Best model fit. *Blue dotted line*: Best fit without the $CH_3D$ lines.

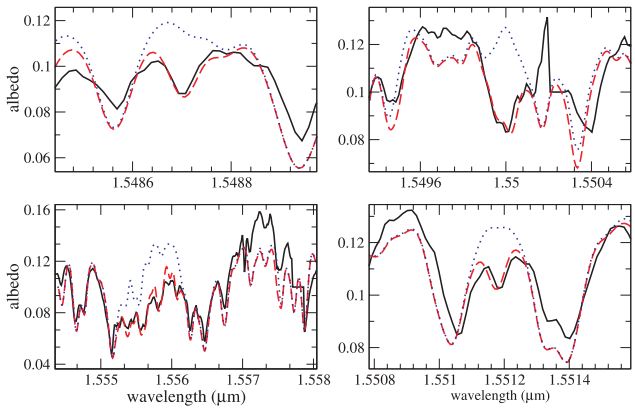


FIG. 2.—Four features that best reveal the absorption from $CH_3D$ distinctively from $CH_4$. *Black solid lines*: Observed spectrum. *Red dashed lines*: Best fit. *Blue dotted lines*: Fit without $CH_3D$ absorption.

quired populations. We modeled the 1.55 $\mu$m spectrum using both the unaltered laboratory line data and the corrected parameters of de Bergh et al. (1988), and we found that without the corrected parameters, a good fit for the whole spectrum was not possible. We also verified that the lines of $^{12}CH_4$ and $^{13}CH_4$ are almost always overlapping, a result of their preserved symmetry. These two isotopes were treated as a single component, with a fixed $^{13}CH_4/^{12}CH_4$ ratio of $1.116 \times 10^{-2}$. To avoid the uncertainties from errors in the identifications and strengths of $CH_4$, we disregarded spectral regions where $CH_3D$ clearly overlaps with strong $CH_4$ features.

The ratio of $CH_4$ to $CH_3D$ was determined from the analysis of stratospheric emission lines of $CH_3D$ and $CH_4$ at 8.6 $\mu$m. We modeled the emission spectrum at 8.6 $\mu$m with a nonscattering LTE model of Titan's atmosphere, which calculates the radiative intensity of the atmosphere from the surface to 450 km altitude, divided into 152 parallel layers. These calculations occur at 8 different air masses, added to obtain the radiance from the whole disk. The line optical depths are calculated assuming Voigt profiles and using the $CH_4$ and $CH_3D$ line parameters of the HITRAN database (Rothman et al. 2003). For this region we also treated $^{13}CH_4$ and $^{12}CH_4$ as a single species with a constant ratio of $1.116 \times 10^{-2}$. We assume the nominal temperature profile of Yelle et al. (1997) and consider variations thereof to evaluate our uncertainties. Haze scattering was not included due to its low efficiency at these wavelengths, which are much larger than the typical particle size. To account for the continuum observed in the data, we included a haze layer of constant optical depth in the lower stratosphere. The optical depth required depends on the assumed temperature profile and thus was adjusted for each temperature profile considered. The uncertainties resulting from this haze layer are incorporated into the temperature-induced uncertainties. We also ran tests using non-LTE source functions (R.V. Yelle 2005, private communication) in atmospheric models extended up to 1300 km altitude and found that the maximum difference between the standard model and the non-LTE model is 2.6%, much smaller than the differences between the fits and the data.

## 4. RESULTS

In Figure 2, we show the separate effects of $CH_4$ and $CH_3D$ for the four best defined features in Titan's spectrum, among which are the two features studied by de Bergh et al. (1988) at 1.550 and 1.556 $\mu$m. Four additional spectral regions at 1.5457, 1.5468, 1.5471, and 1.5586 $\mu$m also display the effects of $CH_3D$, yet these are strongly contaminated by the $CH_4$ bands and thus are considered unreliable. Two other features, at 1.5517 and 1.5591 $\mu$m, also show $CH_4$ contributions, although not as strong. The best defined four spectral regions (1.5487, 1.5500, 1.5512, and 1.5555$\mu$m, shown in Fig. 2) result in an abundance of (2.0–2.2) $\times 10^{-3}$ km amagat. The uncertainties are caused mainly by the $CH_4$ absorption, dominating those from the haze scattering and surface albedo.

Emission lines at 8.6 $\mu$m are highly sensitive to the atmospheric temperature; therefore, we chose lines that are formed at similar altitudes in Titan's stratosphere. We found that the observed weak and strong lines could not be well fit simultaneously with a single temperature profile, suggesting that the spectrum manifests spatial variations in Titan's thermal profile across the moon's disk. We find that variations in the temperature by $\pm 5$ K introduce an error of 10% in the derived ratio. Figure 1 shows the reduced Titan spectrum at 1155 cm$^{-1}$ (8.6 $\mu$m), along with the best-fit model and a model that excludes $CH_3D$ lines. A total of 36 strong, well-defined individual lines were identified, with 10 due to $CH_4$ and 26 to $CH_3D$.

We find the best fit includes haze at altitude 120 km and optical depth 0.05, although our observations do not strongly constrain simultaneously the haze altitude and optical depth. Our observations indicate a $CH_3D/CH_4$ ratio of $(50 \pm 5) \times 10^{-5}$ assuming our nominal temperature profile. The errors correspond to uncertainties of $\pm 5$ K. Additional uncertainties arising from the 1 $\sigma$ noise level and considering the fits to different line strengths provide an additional uncertainty, with a resulting range of $(50 \pm 10) \times 10^{-5}$.

## 5. DISCUSSION

We derive an integrated $CH_3D$ column abundance of $(2.1 \pm 0.1) \times 10^{-3}$ km amagat. This value agrees with the prior measurement of $1.4^{+1.4}_{-0.7} \times 10^{-3}$ km amagat (de Bergh et al. 1988) from lower resolution spectra. Our derived $CH_3D/CH_4$ ratio of $(50 \pm 10) \times 10^{-5}$ agrees with prior measurements by de Bergh et al. (1988), Coustenis et al. (1989, 2003), and Orton (1992), while differing significantly from the early near-infrared results (Gillet 1975; Kim & Caldwell 1982; see Table 1).

Fouchet & Lellouch (2000) found that fractionation by methane condensation in Titan's atmosphere does not cause a de-

tectable $CH_3D/CH_4$ variation. Thus, the stratospheric isotopic ratio derived here combined with the $CH_3D$ column abundance indicates a total $CH_4$ column abundance of $4.2^{+1.3}_{-0.9}$ km amagat, $4.9^{+1.5}_{-1.0}$% of the total atmospheric column abundance. An atmosphere with 100% saturation in the troposphere and a constant mixing ratio above the tropopause has a column abundance of $4^{+1.4}_{-0.9}$ km amagat (considering tropospheric temperature uncertainties as determined by Lellouch et al. 1989). We find the best fit has a surface $CH_3D$ mixing ratio of (3.0–3.8) $\times$ $10^{-5}$, which corresponds to a methane mixing ratio of 5.0%–9.5% (47%–90% relative humidity with the nominal surface temperature or 37%–109% with the surface temperature range of 92.5–95.7 K). It should be noted that the $CH_3D$ absorption analyzed here is most indicative of the total column abundance and does not constrain well its vertical distribution.

Our results of $4.2^{+1.3}_{-0.9}$ km amagat are consistent with the maximum estimated by Lemmon et al. (2002), of 3.5 km amagat, but do not agree with their estimate of 2.63 $\pm$ 0.17 km amagat. Perhaps this incongruity results from the greater transparency of the atmosphere in the wavelength region that we analyzed, along with the availability of line parameters for $CH_3D$ and a more detailed model of the multiple scattering. Our results do not exclude a saturated atmosphere that never exceeds saturation by more than a few percent, nor do they exclude an atmosphere that achieves high levels of supersaturation in the middle troposphere with subsaturation near Titan's surface, as suggested by the *Voyager* IRIS data (Courtin et al. 1995). It should be noted that some of the differences in the methane column abundance might be the result of seasonal variations on Titan, combined with the different latitude ranges sampled in each study. Which profile presently pertains to Titan's equatorial region will be determined by the GCMS on the *Huygens Probe* (Niemann et al. 2002). The main uncertainty in our derived $CH_3D/CH_4$ ratio results from the variable temperature field across Titan's disk. Better constraints on Titan's temperature profile and its spatial variations will be obtained from spatially resolved IR spectra obtained with *Cassini*'s Composite Infrared Spectrometer (CIRS; Flasar et al. 2004) coupled with *Cassini* radio occultation measurements (Kliore et al. 2004) and *Huygens*' deceleration measurements by the *Huygens* Atmospheric Structure Instrument (Fulchignoni et al. 2002). The first measurements from the CIRS spectra (Flasar et al. 2005) indicate a stratospheric methane mixing ratio of 1.6% $\pm$ 0.5% and horizontal temperature variations of up to 20 K at 1.8 mbar (~160 km), compatible with the range used for our fits. In addition, we note that the D/H ratio will be measured indirectly by the CIRS spectra and directly by the *Huygens* GCMS.

The methane profile in Titan's atmosphere not only indicates the conditions under which clouds form but also, together with the thermal profile, reveals the stability of the atmosphere against convection. For example, with a surface humidity less than 40%, surface convection never releases enough latent heat to render parcels buoyant. The formation of deep convective plumes from the surface to the upper troposphere, where clouds are observed, is not then possible. If supersaturation is necessary for condensation, then the limiting surface humidity needed for high convective plumes is larger.

We thank John Rayner for the CSHELL observations and Matthew Richter for the TEXES observations. We thank Barry Lutz for access to the line parameters data on $CH_3D$ lines, Glenn Orton for access to previous observations, and Roger Yelle for the non-LTE calculations. We also thank Chris McKay for valuable discussions. Paulo Penteado is sponsored by the NASA Planetary Astronomy Program and the Brazilian Government through CAPES. Caitlin Griffith is supported by the NASA Planetary Astronomy Program. Thomas Greathouse and John Rayner were Visiting Astronomers at the Infrared Telescope Facility, which is operated by the University of Hawaii under cooperative agreement NCC 5-538 with the National Aeronautics and Space Administration, Office of Space Science, Planetary Astronomy Program. Thomas Greathouse was supported by SOFIA through USRA grant 8500-98-008 and by the LPI, which is operated by USRA under NASA CAN-NCC5-679.

## REFERENCES

Brown, M. E., Bouchez, A. H., & Griffith, C. A. 2002, Nature, 420, 795
Boussin, C., Lutz, B. L., de Bergh, C., & Hamdouni, A. 1998, J. Quant. Spectrosc. Radiat. Transfer, 60, 501
Boussin, C., Lutz, B. L., Hamdouni, A., & de Bergh, C. 1999, J. Quant. Spectrosc. Radiat. Transfer, 63, 49
Campbell, D. B., Black, G. J., Carter, L. M., & Ostro, S. J. 2003, Science, 302, 431
Courtin, R., Gautier, D., & McKay, C. P. 1995, Icarus, 114, 144
Coustenis, A., Bézard, B., & Gautier, D. 1989, Icarus, 82, 67
Coustenis, A., Salama, A., Schulz, B., Ott, S., Lellouch, E., Encrenaz, T. H., Gautier, D., & Feuchtgruber, H. 2003, Icarus, 161, 383
de Bergh, C., Chauville, J., Lutz, B. L., Owen, T., & Brault, J. 1986, ApJ, 311, 501
de Bergh, C., Lutz, B. L., Owen, T., & Chauville, J. 1988, ApJ, 329, 951
Fink, U., & Larson, H. P. 1979, ApJ, 233, 1021
Flasar, F. M., et al. 2004, Space Sci. Rev., 115, 169
———. 2005, Science, 308, 975
Fouchet, T., & Lellouch, E. 2000, Icarus, 144, 114
Fulchignoni, M., et al. 2002, Space Sci. Rev., 104, 395
Gillet, F. 1975, ApJ, 201, L41
Greene, T. P., Tokunaga, A. T., Toomey, D. W., & Carr, J. B. 1993, Proc. SPIE, 1946, 313
Griffith, C. A., Hall, J. L., & Geballe, T. R. 2000, Science, 290, 509
Griffith, C. A., Owen, T., Miller, G. A., & Geballe, T. 1998, Nature, 395, 575
Karkoschka, E. 1998, Icarus, 133, 134
Kim, S. J., & Caldwell, J. 1982, Icarus, 52, 473
Kliore, A. J., et al. 2004, Space Sci. Rev., 115, 1
Lacy, J. H., Richter, M. J., Greathouse, T. K., Jaffe, D. T., & Zhu, Q. 2002, PASP, 114, 153
Lellouch, E., Coustenis, A., Gautier, D., Raulin, F., Dubouloz, N., & Frere, C. 1989, Icarus, 79, 328
Lellouch, E., Coustenis, A., Maillard, J.-P., Strong, K., Deme, N., Griffith, C., & Schmitt, B. 1992, in ESA Symp. on Titan, ed. B. Kaldeich (ESA SP-338; Noordwijk: ESA), 353
Lemmon, M. T., Smith, P. H., & Lorenz, R. D. 2002, Icarus, 160, 375
Lutz, B. L., de Bergh, C., & Maillard, J. P. 1983, ApJ, 273, 397
McKay, C. P., Pollack, J. B., & Courtin, R. 1989, Icarus, 80, 23
———. 1991, Science, 253, 1118
Niemann, H. B., et al. 2002, Space Sci. Rev., 104, 553
Orton, G. 1992, in ESA Symp. on Titan, ed. B. Kaldeich (ESA SP-338; Noordwijk: ESA), 81
Roe, H. G., de Pater, I., Macintosh, B. A., & McKay, C. P. 2002, ApJ, 581, 1399
Rothman, L. S., et al. 2003, J. Quant. Spectrosc. Radiat. Transfer, 82, 5
Samuelson, R. E. 1983, Icarus, 53, 364
Stamnes, K., Tsay, S.-C., Jayaweera, K., & Wiscombe, W. 1988, Appl. Opt., 27, 2502
Trafton, L. 1975, ApJ, 195, 805
Yelle, R. V., Strobel, D. F., Lellouch, E., & Gautier, D. 1997, in *Huygens*: Science, Payload and Mission, ed. A. Wilson (ESA SP-1177; Noordwijk: ESA), 243